CrossMark

Organic dyes containing fluorenylidene functionalized phenothiazine donors as sensitizers for dye sensitized solar cells

Ankita Saini[1] · K. R. Justin Thomas[1] · Chun-Ting Li[2] · Kuo-Chuan Ho[2]

Abstract Two new organic sensitizers featuring fluorenylidene decoration on the phenothiazine donor have been synthesized and characterized as sensitizers for nanocrystalline TiO_2-based dye sensitized solar cells (DSSCs). The dyes possess cyanoacrylic acid as acceptor/ anchoring group and a conjugation pathway composed of fluorene and thiophene. Introduction of the fluorenylidene moiety on phenothiazine enhances the optical density of the dyes while the extension of conjugation by thiophene insertion red-shifts the absorption peak originating from the intramolecular charge transfer from phenothiazine to cyanoacrylic acid. The ground and excited state oxidation potentials of the fluorenylidene-containing dyes are upwardly shifted when compared to the parent dyes indicating a π-delocalized donor segment. The electronic properties were supported by density functional theoretical computations. Among the DSSCs fabricated, the dye (**5a**) having fluorene and thiophene in the spacer resulted higher power conversion efficiency (3.31 %) than the corresponding bithiophene analog (**5b**, 2.83 %) attributable to the relatively high electron life time and enhanced resistance for recombination in the former.

✉ K. R. Justin Thomas
krjt8fcy@iitr.ac.in

[1] Organic Materials Laboratory, Department of Chemistry, Indian Institute of Technology Roorkee, Roorkee 247667, India

[2] Department of Chemical Engineering, National Taiwan University, Taipei 10617, Taiwan

1 Introduction

Due to ever increasing energy crisis, research efforts are directed to tap alternative renewable energy sources because of its easy availability and cost efficiency. Among the renewable energy sources, photovoltaic technology is the best and facile to implement. Despite the commercial progress with silicon-based photovoltaic cells dye sensitized solar cells (DSSCs) [1] invented by Grätzel have received immense attention due to its low cost, easy fabrication, structural flexibility, transparency and high power conversion efficiency (PCE) [2]. Investigations to optimize the various components of DSSCs such as electrodes, electrolyte, sensitizers and TiO_2 have been undertaken in recent years [3]. Although a number of metal oxides with different morphologies are in use as photoanode [4, 5] TiO_2 and ZnO-based [6–8] photoanodes are attractive. However, DSSCs based on TiO_2 are more efficient than ZnO-based devices majorly due to the large surface area exhibited by TiO_2 and instability of ZnO in acidic dye solutions. As a result the best efficiency for ZnO based solar cells (5 %) is still far lower than that for TiO_2 (11 %). In 1981, Matsumura et al. [9] and Alonso et al. [10] used rose bengal and related dyes adsorbed on sintered ZnO and demonstrated efficiency <1 %. Later Grätzel et al. [11] introduced TiO_2 electrodes for inorganic dye sensitizer exhibiting 44 % incident photon to current conversion efficiency. Particularly, sensitizers play a vital role in the performance of DSSCs since it is the main tool to harvest the solar flux. Both inorganic and organic sensitizers have been demonstrated successfully. Organic sensitizers possess large molar absorption coefficients in the visible region, and their functionalization can be performed through simple chemical routes [2, 12–16]. Therefore, organic dyes possessing several structural configurations and functional chromophores have been explored. Apart from the most
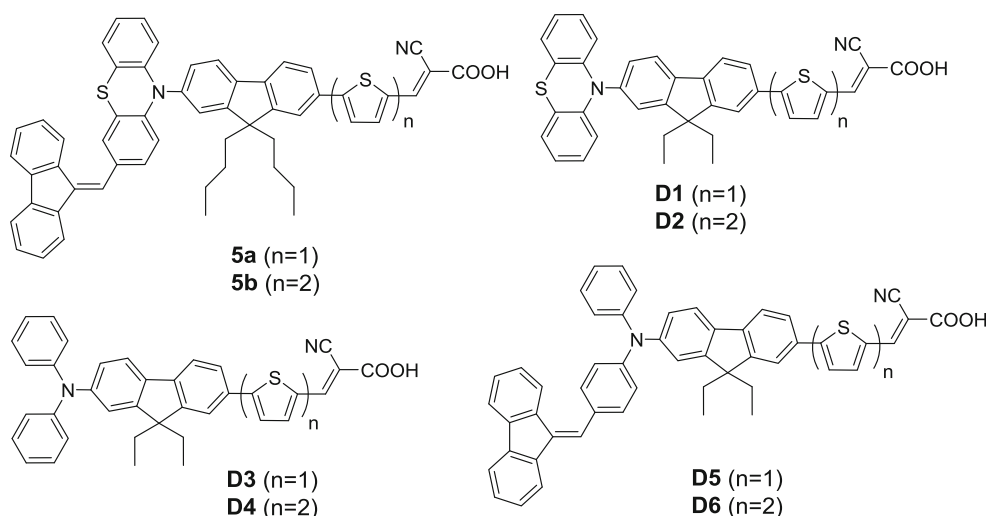
Fig. 1 Structures of the dyes

basic donor–π-bridge–acceptor (D–π–A) [17, 18] architecture, formulations containing auxiliary donors (D–π–D–A) [19, 20], and additional acceptor (D–π–A–π–A) [21, 22] have also been explored. Various donor groups such as triarylamine [17, 18, 23–26], indoline [27, 28], carbazole [29–33], phenothiazine [19, 34–38], and dithienopyrrole [39–41] with different conjugating bridges and cyanoacrylic acid acceptor have been synthesized for application in dye-sensitized solar cells. However, the efficiencies of DSSCs using organic sensitizers are slightly inferior to those employing organometallic dyes such as ruthenium-polypyridyl complexes [3]. This can be attributed to the π-stacking interaction between the dye molecule that leads to aggregate formation on TiO₂ surface and enhances dark current that decreases overall efficiency of the DSSCs [3].

In this work we have conveniently coupled fluorene [26, 35, 42–44], phenothiazine and fluorenylidene [26] to act as electron rich moieties in framing organic sensitizers. Both fluorene and phenothiazine have been extensively used in several organic dyes for OLEDs and DSSCs. We have incorporated fluorene as aromatic π-linker and as a peripheral chromophore due to its rigidity which facilitates effective electron delocalization [42]. While butterfly shaped phenothiazine prevent aggregation of dyes due to its nonplanar structural arrangement [45]. Phenothiazine can be functionalized through its active C-3 and/or N-10 position to use it as lateral or orthogonal chromophore. We have particularly functionalized phenothiazine through its N-10 position to have perpendicular oriented donating group. Although this orientation hampers the donor–acceptor interaction in dyes **D1**–**D2** as illustrated by Thomas et al. previously [35]. While, on the other hand it helps to prevent the approach of I₃⁻ towards conduction band of the

semiconductor and hence accelerates the performance in DSSCs. Also, Thomas et al. [26] have reported that fluorenylidene on dyes **D5**–**D6** helped to delocalize the positive charge generated on the amine unit on removal of electrons when compared to parent dyes **D3**–**D4**. Also it helped to reduce the back electron transfer from the TiO₂ conduction band to oxidized dye. It is interesting to study the effect of replacing fluorenylidene functionalized diphenylamine donor with that of phenothiazine. Phenothiazine is electron-rich when compared to diphenylamine unit due to the presence of sulfur. This may help to fine tune the HOMO and LUMO levels of the resulting dyes.

Herein, we have synthesized two D–π–A sensitizers (Fig. 1, **5a** and **5b**) featuring fluorenylidene functionalized phenothiazine donor, fluorenylthiophene linker and cyanoacrylic acid as acceptor/anchoring group. We have studied the effect of addition of weak electron-withdrawing fluorenylidene on orthogonally oriented phenothiazine as well as the nature of the conjugation bridge on the optical and electrochemical properties. The presence of this peripheral chromophore severely affected the electronic structure and altered the performance of the dye in TiO₂-based DSSC. A comparative evaluation on the parent dyes known in the literature is presented.

2 Experimental section

2.1 Characterization and instrumentation

The ¹H and ¹³C NMR spectra were obtained from either a Bruker 500 MHz or JEOL 400 MHz spectrometers. Mass spectra were recorded in positive-ion mode on a Bruker ESI

TOF high-resolution mass spectrometer. Electronic absorption spectra were obtained on a Cary 100 UV–visible spectrophotometer using freshly prepared solutions. Cyclic voltammetric experiments were carried out at room temperature in dichloromethane using 0.1 M tetrabutylammonium perchlorate as supporting electrolyte. The three-electrode configuration contained a glassy carbon working electrode, a platinum wire counter electrode, and a nonaqueous Ag/AgNO$_3$ reference electrode. The $E_{1/2}$ values were determined as $1/2(E_p^a + E_p^c)$, where E_p^a and E_p^c are the anodic and cathodic peak potentials, respectively. The potentials are quoted against the ferrocene internal standard.

2.2 Device fabrication and characterization of DSSC

The device fabrication and characterization method was same as earlier reported for dyes from our laboratory [39]. Some important details are provided here. The photoanode was prepared by coating transparent (20 nm TiO$_2$ with $\sim$12 μm thickness) and scattering (300 nm TiO$_2$ with $\sim$4 μm thickness) layers by doctor blade method on a pretreated fluorine-doped SnO$_2$ conducting glass (FTO, 7 Ω sq.$^{-1}$, transmittance $\sim$80 %, NSG America, Inc., New Jersey, USA). The dyes were adsorbed by immersing above photoanode in a 3×10^{-4} M dye solution for 24 h, at room temperature. A solvent mixture containing acetonitrile, *tert*-butyl alcohol and dimethyl sulfoxide (volume ratio of 3.5:3.5:3) was used to prepare the dye solution. A mixture of 1-propyl-2,3-dimethylimidazolium iodide (1.2 M), iodine (0.035 M), *tert*-butylpyridine (0.5 M) and guanidine thiocyanate (0.1 M) dissolved in acetonitrile/3-methoxypropionitrile mixture (8:2) served as electrolyte. The active area of the DSSC was restricted to 0.16 cm^2 by using a mask.

2.3 Computational methods

All the computations were performed using Gaussian 09 program package [46]. The ground-state geometries were fully optimized without any symmetry constraints using DFT employing M062x [47] hybrid correlation functional with 6-31G (d,p) basis set for all atoms. Vibrational analysis on the optimized structures was performed to confirm the structure of the compounds. The excitation energies and oscillator strengths for the lowest 10 singlet–singlet transitions at the optimized geometry in the ground state were obtained by TD-DFT calculations using DGDZVP [48, 49] basis set with M062x hybrid functional.

2.4 Synthetic details

All the reactions were performed under nitrogen atmosphere by following standard inert atmosphere procedures.

Solvents were dried by following standard procedures and distilled freshly from the corresponding drying agent prior to use. All column chromatography purifications were performed using 100–200 mesh silica gel as the stationary phase in a column measuring 30 cm long and 2.0 cm diameter. 10-(7-Bromo-9,9-dibutyl-9*H*-fluoren-2-yl)-10*H*-phenothiazine (**1**) was synthesized according to the literature procedure [35].

2.4.1 10-(7-Bromo-9,9-dibutyl-9H-fluoren-2-yl)-10H-phenothiazine-3-carbaldehyde (2)

In a 50 mL flask, 10-(7-bromo-9,9-dibutyl-9H-fluoren-2-yl)-10*H*-phenothiazine (**1**, 2 g, 3.6 mmol), chloroform (5 mL) and DMF (10 mL) were taken and cooled to 0 °C by immersion in ice bath. To the cold solution was added POCl$_3$ (2.1 mL, 22 mmol) drop-wise with vigorous stirring over 1 h. After the addition, the reaction temperature was raised to 100 °C and kept at this condition for 18 h. After completion of reaction, it was then poured into ice water and neutralized with aqueous sodium hydroxide. The precipitates formed were extracted with chloroform and the extracts dried over anhydrous Na$_2$SO$_4$. The concentrate was adsorbed on silica gel and purified by column chromatography by using hexane/CHCl$_3$ (1:1) as eluent. Yellow solid; yield 1.6 g (76 %); mp 182–184 °C; IR (KBr, cm^{-1}) 1680.03 ($\nu_{C=O}$); ^{1}HNMR (CDCl$_3$, 500.13 MHz) δ 9.70 (s, 1H), 7.93 (d, J = 8.5 Hz, 1H), 7.63 (d, J = 8.5 Hz, 1H), 7.52–7.54 (m, 2H), 7.48 (d, J = 2.0 Hz, 1H), 7.32–7.33 (m, 2H), 7.25 (d, J = 1.5 Hz, 1H), 6.99 (dd, J = 7.5 Hz, 1.5 Hz, 1H), 6.79–6.87 (m, 2H), 6.20 (d, J = 8.5 Hz, 1H), 6.15 (d, J = 8.0 Hz, 1H), 1.95–2.00 (m, 4H), 1.03–1.15 (m, 4H), 0.57–0.70 (m, 10 H); ^{13}CNMR (CDCl$_3$, 125.75 MHz) δ 191.0, 154.9, 154.6, 150.6, 144.1, 142.3, 140.29, 140.26, 132.4, 131.8, 131.1, 130.8, 128.9, 128.4, 128.1, 127.8, 126.8, 125.1, 123.7, 123.4, 122.9, 121.3, 120.3, 117.6, 116.2, 57.1, 41.2, 27.5, 24.2, 15.2; HRMS calcd for C$_{34}$H$_{32}$BrNOS [M] m/z 581.1382, found 581.1376.

2.4.2 3-((9H-Fluoren-9-ylidene)methyl)-10-(7-bromo-9,9-dibutyl-9H-fluoren-2-yl)-10H-phenothiazine (3)

The compounds 10-(7-bromo-9,9-dibutyl-9H-fluoren-2-yl)-10*H*-phenothiazine-3-carbaldehyde (**2**) (1.6 g, 2.75 mmol) and 9*H*-fluorene (0.46 g, 2.75 mmol) were suspended in 20 mL ethanol. Sodium ethoxide (5 eq) solution was added to it with vigorous stirring. It was refluxed for 12 h. An orange red solid was formed. It was filtered and washed with cold methanol and water. The dried sample was found to be analytically pure. Yield 1.4 g (70 %); mp

162–164 °C; ^{1}HNMR (CDCl$_3$, 500.13 MHz) δ 7.94 (d, $J = 5.5$ Hz, 1H), 7.83 (d, $J = 8.0$ Hz, 1H), 7.69–7.74 (m, 3H), 7.64 (d, $J = 9.0$ Hz, 1H), 7.52 (s, 2H), 7.39–7.45 (m, 3H), 7.28–7.37 (m, 4H), 7.12 (t, $J = 7.5$ Hz, 1H), 7.04 (d, $J = 7.0$ Hz, 2H), 6.83 (br s, 2H), 6.22 (br s, 2H), 1.96–2.05 (m, 4H), 1.05–1.17 (m, 4H), 0.62–0.75 (m, 10H); ^{13}CNMR (CDCl$_3$, 100.53 MHz) δ 153.6, 153.5, 144.4, 144.2, 141.3, 140.7, 139.8, 139.3, 139.1, 137.5, 136.6, 135.8, 131.1, 130.5, 129.9, 128.6, 128.5, 128.2, 127.8, 127.1, 127.0, 126.9, 126.9, 126.5, 126.3, 126.03, 125.1, 124.5, 122.9, 122.3, 122.0, 121.6, 120.3, 120.2, 119.9, 119.7, 119.4, 115.9, 115.4, 100.2, 55.9, 40.1, 29.9, 26.4, 23.1, 14.1; HRMS calcd for C$_{47}$H$_{40}$BrNS [M + Na] m/z 752.1957, found 752.1932.

2.4.3 5-(7-(3-((9H-Fluoren-9-ylidene)methyl)-10H-phenothiazin-10-yl)-9,9-dibutyl-9H-fluoren-2-yl)thiophene-2-carbaldehyde (4a)

A mixture of (5-(1,3-dioxolan-2-yl)thiophen-2-yl)tributyl-stannane (0.286 g, 0.55 mmol), 3-((9H-fluoren-9-yli-dene)methyl)-10-(7-bromo-9,9-dibutyl-9H-fluoren-2-yl)-10H-phenothiazine (3) (0.365 g, 0.5 mmol), Pd(PPh$_3$)$_2$Cl$_2$ (4 mg, 0.005 mmol) and DMF (3 mL) was heated at 80 °C for 24 h. After the completion of reaction, it was poured into cold water and extracted with CHCl$_3$, washed thoroughly with brine solution and dried over Na$_2$SO$_4$. The volatiles were removed by vacuum evaporation using rotary evaporator to yield an orange residue. It was taken in glacial acetic acid (5 mL) and heated at 60 °C for 1 h to form a clear solution. After 1 h, 15 mL water was added and heated at 60 °C for further 4 h. The cold reaction mixture was extracted with CHCl$_3$. The CHCl$_3$ extract was washed thoroughly with brine solution and dried over anhydrous Na$_2$SO$_4$. The solid obtained on evaporation of the solvent was purified by column chromatography on silica gel using hexane/dichloromethane mixture (3:2) as an eluent. Orange solid; yield 0.33 g (87 %); mp 154–156 °C; IR (KBr, cm^{-1}) 1662.10 ($v_{C=O}$); ^{1}HNMR (CDCl$_3$, 500.13 MHz) δ 9.92 (s, 1H); 8.00 (d, $J = 8.0$ Hz, 1H), 7.81–7.84 (m, 2H), 7.79 (d, $J = 4.0$ Hz, 1H), 7.72–7.75 (m, 2H), 7.68–7.71 (m, 3H), 7.51 (d, $J = 4.0$ Hz, 1H), 7.45–7.48 (m, 3H), 7.28–7.36 (m, 3H), 7.04–7.14 (m, 4H), 6.83–6.86 (m, 2H), 6.22–6.26 (m, 2H), 2.04–2.08 (m, 4H), 1.08–1.14 (m, 4H), 0.67–0.73 (m, 10H); ^{13}CNMR (CDCl$_3$, 100.53 MHz) δ 182.9, 154.9, 154.3, 152.4, 144.4, 144.2, 141.8, 141.3, 140.7, 140.1, 137.7, 132.6, 131.1, 130.1, 128.6, 128.5, 128.2, 127.8, 127.1, 127.05, 127.01, 126.96, 126.91, 126.3, 126.1, 126.0, 124.5, 124.3, 122.9, 122.7, 120.97, 120.93, 120.3, 120.2, 119.9, 119.7, 115.9, 115.4, 55.8, 40.2, 31.5, 26.4, 23.1, 14.1; HRMS calcd for C$_{52}$H$_{43}$NOS$_2$ [M] m/z 761.2780, found 761.2761.

2.4.4 5-(5-(7-(3-((9H-Fluoren-9-ylidene)methyl)-10H-phenothiazin-10-yl)-9,9-dibutyl-9H-fluoren-2-yl)thiophen-2-yl)thiophene-2-carbaldehyde (4b)

It was prepared by following a procedure described above for the compound 4a but using (5-(5-(1,3-dioxolan-2-yl)thiophen-2-yl)thiophen-2-yl)tributylstannane (0.682 g, 1.1 mmol) and 3-((9H-fluoren-9-ylidene)methyl)-10-(7-bromo-9,9-dibutyl-9H-fluoren-2-yl)-10H-phenothiazine (3). Dark red solid; yield 0.62 g (73 %); mp 118–120 °C; IR (KBr, cm^{-1}) 1658.33 ($v_{C=O}$); ^{1}HNMR (CDCl$_3$, 500.13 MHz) δ 9.88 (s, 1H), 7.98 (d, $J = 8.0$ Hz, 1H), 7.84 (d, $J = 8.0$ Hz, 1H), 7.79 (d, $J = 8.0$ Hz, 1H), 7.65–7.72 (m, 5H), 7.61 (d, $J = 8.0$ Hz, 1H), 7.40–7.47 (m, 2H), 7.37–7.39 (m, 2H), 7.33–7.36 (m, 2H), 7.29–7.32 (m, 3H), 7.03–7.12 (m, 4H), 6.83–6.86 (m, 2H), 6.23–6.27 (m, 2H), 2.03–2.08 (m, 4H), 1.06–1.16 (m, 4H), 0.68–0.74 (m, 10H); ^{13}CNMR (CDCl$_3$, 100.53 MHz) δ 182.7, 154.1, 152.3, 147.3, 146.8, 144.4, 144.2, 141.7, 141.3, 141.0, 140.6, 139.8, 139.7, 139.1, 137.7, 136.0, 135.7, 135.2, 133.1, 130.9, 129.9, 128.6, 128.5, 128.2, 127.8, 127.4, 127.1, 126.9, 126.9, 126.4, 126.0, 125.3, 124.5, 124.2, 122.9, 122.4, 120.9, 120.3, 120.22, 120.15, 119.9, 119.7, 119.6, 119.4, 115.9, 115.4, 55.8, 40.2, 29.4, 23.1, 14.2; HRMS calcd for C$_{56}$H$_{45}$NOS$_3$ [M + H] m/z 844.2736, found 844.2706.

2.4.5 (E)-3-(5-(7-(3-((9H-Fluoren-9-ylidene)methyl)-10H-phenothiazin-10-yl)-9,9-dibutyl-9H-fluoren-2-yl)thiophen-2-yl)-2-cyanoacrylic acid (5a)

A mixture of 5-(7-(3-((9H-fluoren-9-ylidene)methyl)-10H-phenothiazin-10-yl)-9,9-dibutyl-9H-fluoren-2-yl)thiophene-2-carbaldehyde (4a) (0.30 g, 0.4 mmol), cyanoacetic acid (51 mg, 0.6 mmol), acetic acid (5 ml) and ammonium acetate (5 mg) was heated at 120 °C for 8 h. The resulting orange red solution was poured into ice-cold water to produce dark orange precipitates. This was filtered and washed thoroughly with water and dried. The solid was further washed with hexane and crystallized from methanol to give orange solid. It was obtained in pure form by recrystallization from hexane/CHCl$_3$. Orange solid (0.13 g, 67 %); mp 258–260 °C; IR (KBr, cm^{-1}) 2216.19 ($v_{C\equiv N}$); ^{1}HNMR (CDCl$_3$, 500.13 MHz) δ 8.39 (s, 1H), 7.99 (d, $J = 8.0$ Hz, 1H), 7.82 (d, $J = 7.0$ Hz, 3H), 7.78 (d, $J = 7.0$ Hz, 1H), 7.69–7.73 (m, 4H), 7.53 (d, $J = 12.0$ Hz, 1H), 7.43–7.46 (m, 4H), 7.29–7.36 (m, 3H), 7.03–7.13 (m, 4H), 6.83–6.85 (m, 2H), 6.22–6.26 (m, 2H), 2.06–2.09 (m, 4H), 1.06–1.15 (m, 4H), 0.66–0.71 (m, 10H); ^{13}CNMR (CDCl$_3$, 100.53 MHz) δ 154.4, 147.9, 141.3, 140.6, 140.3, 139.8, 139.11 131.10, 130.06, 128.6, 128.5, 128.2, 127.9, 127.3, 127.1, 127.0, 126.9, 126.32, 126.28, 126.1, 124.8, 124.5, 122.9, 122.8, 121.0, 120.9, 120.3, 119.9, 119.8, 115.9, 115.4, 55.9, 40.1, 26.4, 23.1, 14.2; HRMS calcd for C$_{55}$H$_{44}$N$_2$O$_2$S$_2$ [M + Na] m/z 851.2736, found 851.2736.

2.4.6 (E)-3-(5-(5-(7-(3-((9H-Fluoren-9-ylidene)methyl)-10H-phenothiazin-10-yl)-9,9-dibutyl-9H-fluoren-2-yl)thiophen-2-yl)thiophen-2-yl)-2-cyanoacrylic acid (5b)

It was obtained from 5-(5-(7-(3-((9H-fluoren-9-yli-dene)methyl)-10H-phenothiazin-10-yl)-9,9-dibutyl-9H-flu-oren-2-yl)thiophen-2-yl)thiophene-2-carbaldehyde (**4b**) (0.30 g, 0.36 mmol), cyanoacetic acid (45 mg, 0.54 mmol) by following the procedure described above for **5a**. Dark red solid; yield 0.13 g (62 %); mp 210–212 °C; IR (KBr, cm^{-1}) 2213.25 ($\nu_{C \equiv N}$); ^{1}HNMR (CDCl$_3$, 500.13 MHz) δ 8.33 (s, 1H), 7.98 (d, $J = 8.0$ Hz, 1H), 7.83 (d, $J = 8.0$ Hz, 1H), 7.80 (d, $J = 8.0$ Hz, 1H), 7.67–7.74 (m, 5H), 7.63 (s, 1H), 7.44–7.47 (m, 2H), 7.41–7.42 (m, 2H), 7.35 (m, 2H), 7.29–7.33 (m, 4H), 7.03–7.14 (m, 4H), 6.83–6.85 (m, 2H), 6.21–6.27 (m, 2H), 2.05–2.09 (m, 4H), 1.09–1.17 (m, 4H), 0.68–0.74 (m, 10H); ^{13}CNMR (CDCl$_3$, 100.53 MHz) δ 152.2, 144.1, 140.9, 140.1, 139.7, 138.9, 136.5, 134.7, 134.1, 132.9, 130.9, 129.8, 128.44, 128.39, 128.1, 127.85, 127.79, 127.71, 127.67, 126.9, 126.9, 126.8, 126.2, 125.9, 125.2, 125.0, 124.6, 124.4, 122.8, 122.3, 120.8, 120.2, 120.0, 119.9, 119.8, 119.7, 119.61, 119.6, 115.8, 115.3, 55.7, 40.1, 26.3, 23.0, 14.1; HRMS calcd for C$_{59}$H$_{46}$N$_2$O$_2$S$_3$ [M + H] m/z 911.2794, found 911.2784.

3 Results and discussion

3.1 Synthesis and characterization

The synthetic pathway of the dyes, **5a** and **5b**, are dis-played in Scheme 1. The precursor 10-(7-bromo-9,9-dibutyl-9H-fluoren-2-yl)-10H-phenothiazine was synthe-sized by a stoichiometrically controlled palladium-cat-alyzed C–N cross-coupling reaction [50] between 2,7-dibromo-9,9-dibutylfluorene and phenothiazine by follow-ing a procedure reported in literature. Subsequently, it was converted to the aldehyde, **2** by Vilsmeier–Haack formy-lation reaction with DMF/POCl$_3$. It was then condensed with 9H-fluorene in the presence of sodium ethoxide to obtain the fluorenylidene derivative (**3**). This precursor was treated with the appropriate tin derivatives of protected thiophene aldehydes under the Stille reaction [51] condi-tions followed by acid hydrolysis to obtain the required aldehydes **4a** and **4b**. Finally, Knoevenagel condensation of aldehyde derivatives with cyanoacetic acid in the pres-ence of ammonium acetate resulted in the fluorenylidene functionalized phenothiazine-based organic dyes, **5a** and **5b**. All compounds were characterized by ^{1}H and ^{13}CNMR and mass spectral methods. The spectral data of the dyes are consistent with the proposed structures. The intensively colored dyes are moderately soluble in common organic solvents such as dichloromethane (DCM), tetrahydrofuran (THF), dimethyl sulfoxide (DMSO), dimethyl formamide (DMF), acetonitrile (ACN), etc.

3.2 Photophysical properties

The absorption spectra of the two new dyes recorded in DCM are displayed in Fig. 2 and the corresponding pho-tophysical data are listed in Table 1. Both the dyes exhibited two distinctive absorption bands. The more prominent red-shifted band appearing in the range of 370–550 nm is attributed to the intramolecular charge-transfer (ICT) from the functionalized phenothiazine donor
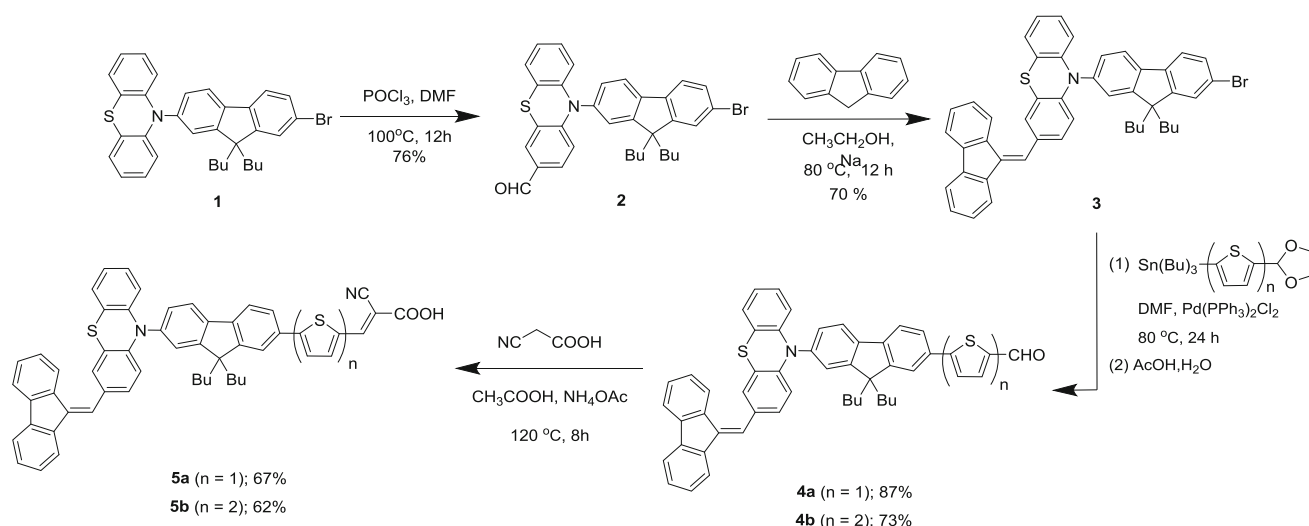
Scheme 1 Synthesis of the dyes
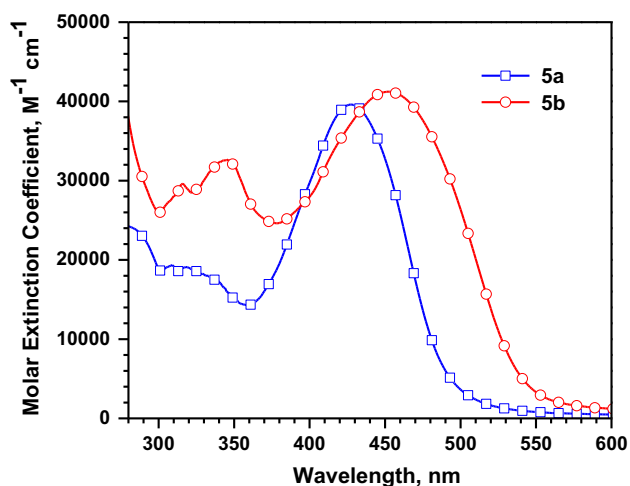
Fig. 2 Absorption spectra of the dyes **5a** and **5b** recorded in DCM solutions

to the cyanoacrylic acid acceptor bridged by fluorene-(thiophene)$_n$ (n = 1 or 2) π-linker. The second less intense absorption band covering the shorter wavelength region of 280–360 nm is due to the localized π–π* transitions in the dye arising from phenothiazine and fluorene [52]. It has been found that the presence of an additional thiophene unit in the conjugation pathway enhances the optical properties. Thus the dye **5b** exhibits a red-shift of 25 nm in the absorption spectra attributed to the increase in the electron richness of the π-linker conjugation. Also, the molar extinction coefficients of the charge transfer transition in both dyes are significantly larger than the ruthenium-based dyes [3, 15]. The introduction of fluorenylidene unit as a peripheral chromophore on the

parent dye **D1** and **D2** helps to increase the molar extinction coefficient which may be beneficial for better light harvesting in DSSCs [26]. It is interesting to compare optical data (Table 1) of these two dyes to that of the reference dyes (**D1–D6**). The present dyes (**5a** and **5b**) exhibit a hypsochromically shifted absorption profiles when compared to the parent dyes **D1** and **D2** which points the weak electron withdrawing character of the fluorenylidene unit. Also, in comparison to dyes **D5** and **D6** possessing diphenylamine instead of phenothiazine (**5a** and **5b**) there is a blue shift in absorption maxima in later attributed to weak electronic coupling between the donor and acceptor as seen for the set of the parent dyes **D1–D4**. This may be due to (1) orthogonally oriented rigid phenothiazine due to the linkage via *N*-10 position, (2) less electronic richness of donor owing to delocalization of electronic density towards fluorenylidene segment. This delocalization of the electron could be enhanced and easily facilitated in present set of dyes (**5a** and **5b**) due to the rigidification and non-favorable orientation of phenothiazine against the π-linker. However, a blue-shift in absorption has been noticed for the dyes **D5** and **D6** when compared to the corresponding parent dyes **D3** and **D4**.

The organic dyes tend to aggregate at TiO_2 surface and result in either bathochromic or hypsochromic shift in the absorption spectrum depending on the type of aggregation [53]. The present dyes when anchored on TiO_2 exhibits broadened and a bathochromically shifted spectra (Fig. 3) as compared to that observed in solution (Fig. 2). This may be due to the large thickness of the TiO_2 film [54] or due to *J*-aggregation of the dye molecules facilitating charge transport across the molecules [53]. However, the spectral trend (**5b** > **5a**) remained similar to that observed in

Table 1 Optical and electrochemical data of the dyes

Dye	λ_{abs},[a] nm (ε_{max}, $M^{-1}cm^{-1} \times 10^3$)[a]	λ_{TiO_2}, nm	E_{ox}, mV (ΔE_p)[b]	HOMO,[c] (eV)	LUMO,[d] (eV)	E_{0-0},[e] (eV)	$E_{ox}*$,[f] (eV)
5a	427 (39.6)	470	253 (60), 873	5.05	2.47	2.58	−1.56
5b	453 (41.2), 346 (32.6)	520	256 (65), 852	5.06	2.55	2.51	−1.48
D1	429 (35.9), 299 (15.8)	445	272 (73)	5.07	2.59	2.48	−1.43
D2	465 (22.7), 345 (14.8)	485	260 (100)	5.06	2.83	2.23	−1.20
D3	469 (34.9), 353 (19.7), 310 (20.8)	471	408 (70)	5.21	3.05	2.16	−0.98
D4	487 (40.5), 371 (26.3), 304 (20.1)	505	313 (63), 745	5.11	3.03	2.09	−1.00
D5	464 (35.5)	466	410 (86), 812	5.21	3.03	2.18	−0.99
D6	470 (38.8)	500	374 (84), 735	5.17	3.04	2.13	−0.99

[a] λ_{abs}, absorption maxima in DCM solution

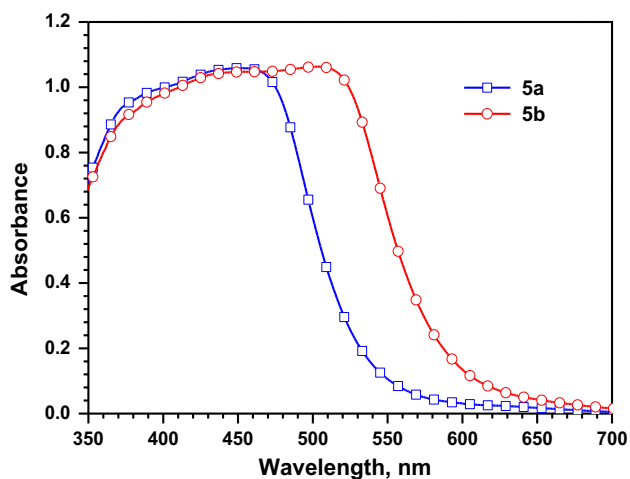[b] Redox potentials are reported with reference to the ferrocene internal standard

[c] Deduced from the oxidation potential using the formula HOMO = 4.8 + E_{ox}

[d] Obtained from the optical band gap and the electrochemically deduced HOMO value

[e] Calculated from optical edge

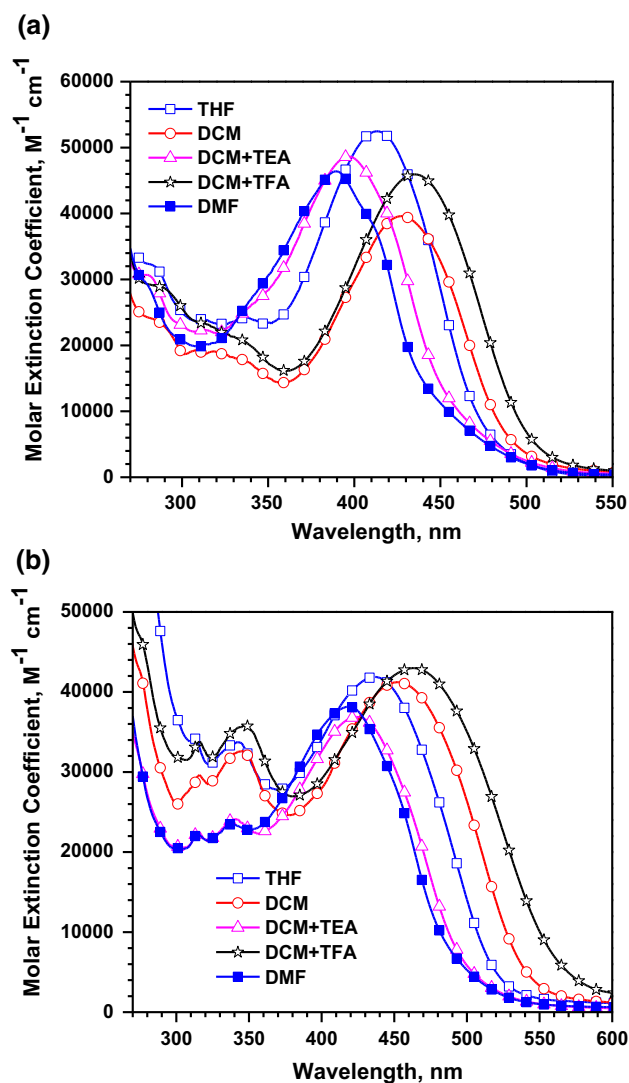[f] Excited-state oxidation potential versus NHE

Fig. 3 Absorption spectra of the dyes recorded on thin TiO$_2$ film

Fig. 4 Absorption spectra of the dye **a** 5a and **b** 5b recorded in different solvents

solution. It is also interesting to compare optical data of the photoanodes of different dyes. Surprisingly, the dyes **5a** and **5b** exhibited red-shifted absorption for the photoanodes when compared to the diphenylamine analogs **D5** and **D6** and the parent dyes **D1** and **D2**. This clearly suggests that the dyes pack in a favorable geometry on the surface of TiO$_2$ and the insertion of the fluorenylidene chromophore on phenothiazine may be beneficial for light harvesting properties.

Further, the presence of acid–base equilibria is confirmed by the addition of small amount of trifluoroacetic acid (TFA) and triethylamine (TEA) to the dye solutions in DCM solutions (Fig. 4; Table S1). For both the dyes exhibited a red-shifted absorption on addition of TFA. While the addition of TEA results in 30 nm hypsochromic shift. This indicates that the dyes are present in a partially deprotonated state in the solution. Therefore, on addition of TFA the equilibrium shifts toward the protonated form and results in a red-shift in the absorption spectra. Whereas the addition of TEA tenders a blue shift as it shifts the equilibrium to the deprotonated form of the dye [55]. Therefore, the response of CT absorption band toward TFA and TEA indicates the alteration of donor- acceptor interactions due to protonation and deprotonation of cyanoacrylic unit.

Since solvent–solute interactions and solvent nature plays an important role in the photophysical behavior of dipolar compounds in solution [56]. The donor–acceptor interactions present in these dyes were further studied by measuring the absorption spectra in THF and DMF. A blue-shift in the absorption spectra of the dyes was observed when recorded in these solvents (Fig. 4). This may be due to the solute–solvent interaction of the dyes in the ground state. It can be correlated to hydrogen bonding in THF which reduces the acceptor strength of carboxylic
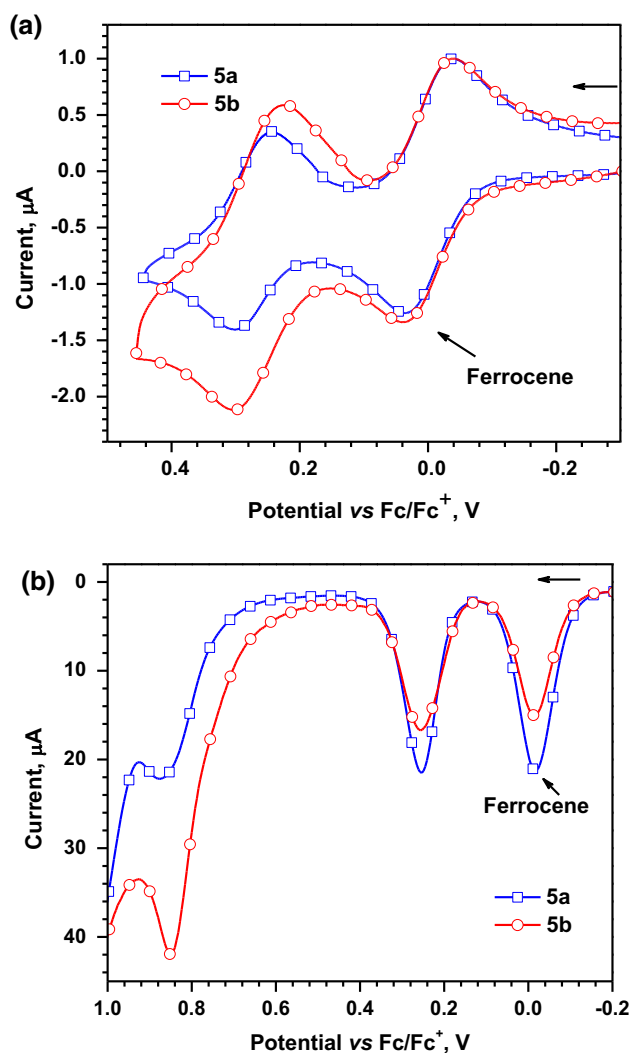
acid unit [57]. In DMF, the equilibrium is probably shifted to the deprotonated form due to the basic nature of solvent [57]. The blue shifted CT band observed in DMF closely resembled to those observed in the presence of TEA. This undoubtedly suggests that the dyes are in the deprotonated state in DMF.
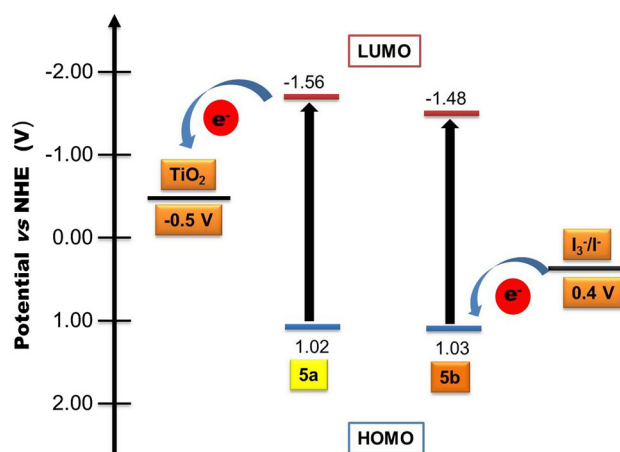
3.3 Electrochemical properties

In order to investigate the redox characteristics of the dyes (Fig. 5; Table 1) cyclic voltammetry (CV) and differential pulse voltammetry (DPV) in DCM solutions were performed. Both the dyes exhibited a reversible oxidation couple (Fig. 5a) attributed to removal of an electron from the phenothiazine donor moiety with redox potential at

(a)

(b)

Fig. 5 **a** Cyclic voltammograms and **b** differential pulse voltammograms of the dyes **5a** and **5b** recorded in DCM solutions

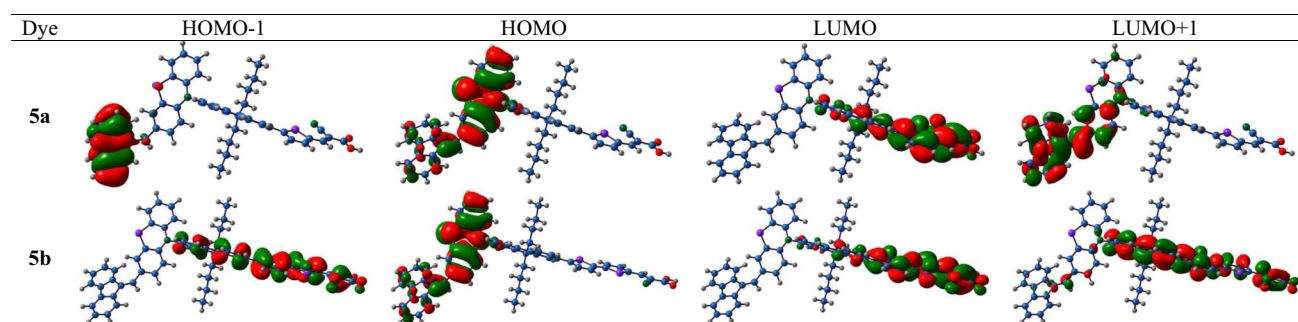**Fig. 6** Energy level diagram of the dyes **5a** and **5b**

still under doubt but can be related to the difference in rigidity and firmness of the electron donating moiety in the above mentioned dyes.

Furthermore, the ground state and excited state energy levels for the dyes were calculated. The thermodynamic driving force for the electron injection and dye regeneration of the dyes in DSSCs is illustrated in energy level diagram (Fig. 6). It was found that the excited state oxidation potentials (E_{ox}*) for the dyes are more negative than the conduction band edge of the TiO_2 (−0.5 V vs NHE) [58]. This facilitates efficient downhill electron injection from the photo-excited dyes into the conduction band of TiO_2. For efficient dye regeneration, the ground-state redox potential of the dye must be more positive than the electrolyte redox potential. The ground state oxidation potentials of the dyes are more positive ($\sim$1.0 V) than the redox potential of I_3^-/I^- electrolyte (0.4 V) [59] which ensures thermodynamically feasible regeneration of the oxidized dyes by the electrolyte.

3.4 Theoretical investigations

To gain further insight into the electronic structure of the dyes, the geometries of the dyes **5a** and **5b** were optimized by density functional theory (DFT) calculations. The optimized geometries were used for calculation of vertical excitation energies using time-dependent density functional theory (TD-DFT). The computed energies of the vertical excitations and their orbital contributions are compiled in Table S2. The electronic distribution in the frontier molecular orbitals HOMO−1, HOMO, LUMO and LUMO+1 of the dyes is shown in Fig. 7. The optimized geometries of the dyes clearly highlight the perpendicular orientation of phenothiazine and fluorene units. The HOMO of the dyes is localized on the phenothiazine unit

$\sim$255 mV vs Fc/Fc$^+$. While an irreversible oxidation peak which is more positive than former peak is observed for both the dyes (Fig. 5b) probably originating from the fluorenyl-thiophene linker. Among the two dyes, dye **5b** possessing bithiophene in the linker shows a lower oxidation potential owing to the enhanced electron density of the conjugation pathway. A similar trend was also observed for the parent dye **D2** on comparison to **D1**. It is interesting to compare diphenylamine-based dyes (**D3** and **D6**) with phenothiazine-based dyes (**5a**, **5b**, **D1** and **D2**). Among the diphenylamine-based dyes (**D3**–**D6**), fluorenylidene containing dyes (**D5** and **D6**) show high first oxidation potentials than the parent dyes (**D3** and **D4**). Whereas, for phenothiazine-based dyes, fluorenylidene functionalized dyes **5a** and **5b** exhibited low oxidation potentials their parent dyes **D1** and **D2**. The appropriate reason for this is

Fig. 7 Electronic distribution in the frontier molecular orbitals of the model compounds **5a** and **5b**

and the LUMO is located on the π-linker cyanoacrylic acid fragment of the dyes. It is worth mentioning that due to configuration of the dyes, poor electronic delocalization hindered facile donor acceptor interactions. This might be the reason for the poor photovoltaic performance of the dyes. However, the trends in the calculated transitions resembled that of experimental observations. The longer wavelength absorption involves the contribution from HOMO−1 to LUMO and HOMO to LUMO+1. Considering the composition of HOMO−1 and LUMO+1 the main observed transition may be described as a charge transfer transition. Interestingly, the major contribution in **5a** is due to the charge transfer from phenothiazine to fluorenylidene. But, the transitions appearing at shorter wavelengths may be ascribed to localized π–π* transitions arising from the phenothiazine and fluorene units.

3.5 Photovoltaic performance of the dyes

Both the dyes were applied as sensitizers in the nanocrystalline TiO_2-based conventional liquid electrolyte DSSC. The photovoltaic performance of the dyes in DSSCs was evaluated by measuring incident photon-to-current conversion efficiency (IPCE) (Fig. 8) and $J–V$ characteristics (Fig. 9). The performance parameters of the DSSCs under standard global AM 1.5 G simulated solar light at a light intensity of 100 mW cm^{-2} are displayed in Table 2. The IPCE spectrum is broad and covers up to 680 nm for the dye **5b** which is consistent with its absorption spectrum. The photocurrent density (J_{SC}) for the dye **5a** is greater than **5b**. This can be attributed to the more broadened and intensified IPCE spectra for the former dye. Furthermore, the high J_{SC} for **5a** is attributable to its high lying LUMO (−1.56 eV). Due to inefficient charge collection efficiency from the excited dye to conduction band of TiO_2, dye **5b** produced comparatively low J_{SC} despite possessing high molar extinction coefficient in absorption spectrum than dye **5a**. Similarly, open circuit voltage (V_{OC}) for the dyes follows the order **5a > 5b**. The larger V_{OC} observed for the
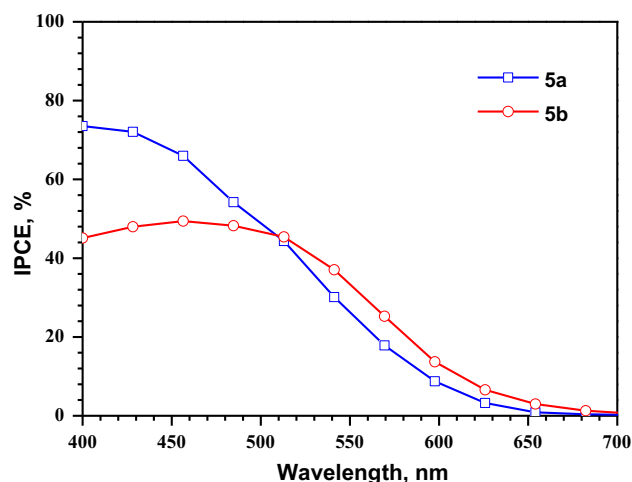
Fig. 8 IPCE plots of the DSSCs fabricated using the dyes
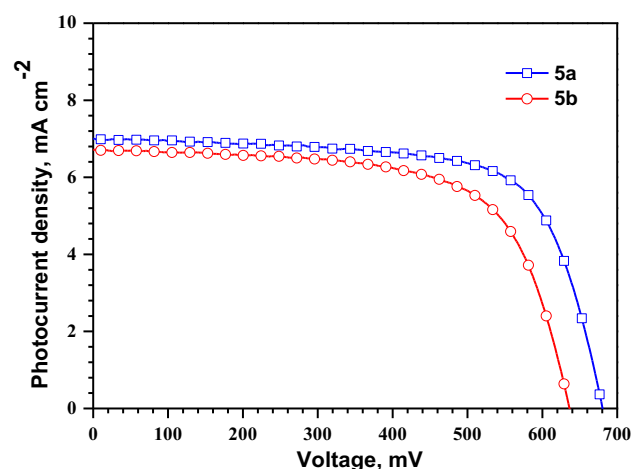
Fig. 9 $J–V$ characteristics of the DSSCs fabricated using the dyes

dye **5a** is because it effectively reduces the possibility of charge recombination by retarding the approach of triiodide ion (I_3^-) at the TiO_2 surface than dye **5b** [35]. The lower open circuit voltage for dye **5b** can be due to the

**Table 2** Performance parameters of the DSSC devices using the dyes

Dye	η (%)	V_{OC} (mV)	J_{SC} (mA cm^{-2})	ff	R_{ct2} (ohm)	τ_e (ms)	R_{rec} (ohm)
5a	3.31	679	7.01	0.70	52.74	2.59	25.49
5b	2.83	635	6.71	0.66	37.93	2.26	23.48
D1	4.47	690	9.36	0.69	25.52	3.43	28.51
D2	4.01	599	10.47	0.64	23.99	1.49	18.55
D3	4.70	690	10.56	0.65	24.83	5.65	61.71
D4	3.01	618	7.52	0.65	33.58	1.41	25.56
D5	5.98	642	14.10	0.66	16.10	8.41	14.50
D6	6.13	650	14.80	0.64	17.07	3.80	31.75

lower resistance to recombination of photoinjected electrons. In general, the lower V_{OC} of a DSSC is attributed to the shorter electron lifetime [60]. Thus, the low efficiency for the device based on the dye **5b** (2.83 %) compared to **5a** (3.31 %) can be attributed to the low-lying LUMO level of the former dye which retards the effective electron injection into the conduction band of TiO$_2$.

It is interesting to compare the photovoltaic characteristics of these two dyes with reference dyes. The performance parameters for **5a** and **5b** follow the same trend as shown by parent dyes **D1** and **D2**. This leads to hampered device efficiency for the present dyes. When compared to diphenylamine-based dyes **D5** and **D6**, the present set of dyes exhibits almost half of the device efficiency. Although dye **5a** possesses a higher V_{OC} than **D5** but due to retarded J_{SC} parameter DSSCs efficiency is decreased. These can be correlated to weaker donor–acceptor interactions in **5a** and **5b** as compared to **D5** and **D6** and enhanced resistance to charge transfer as observed in photo-physical properties.

3.6 Electrochemical impedance spectroscopy

The effect of the dyes on the electron transport and its kinetics at the interfaces in the DSSCs can be estimated with the aid of electrochemical impedance spectroscopy (EIS) measurements. These EIS measurements were carried out under forward bias in dark and 1 sun illumination conditions and corresponding Nyquist plots are displayed as Fig. 10a, b respectively. In general, the EIS spectrum of DSSCs having a configuration FTO/TiO$_2$/dye/electrolyte/Pt/ITO displays three semicircles. The three semicircles corresponds to the resistance for the different electron transfer processes at the TiO$_2$ (R_{ct2}), TiO$_2$/dye/electrolyte/interface (R_{rec}) and Warburg diffusion process of electrolyte (Z_w) in DSSCs. The radius of middle semicircle is the measure of resistance to charge recombination. Generally, bigger is the radius larger is the resistance to the related process. In the Nyquist plots under dark, two semicircles are observed. The R_{rec} obtained from radius of bigger semicircle follows the order **5a** > **5b**. This trend is
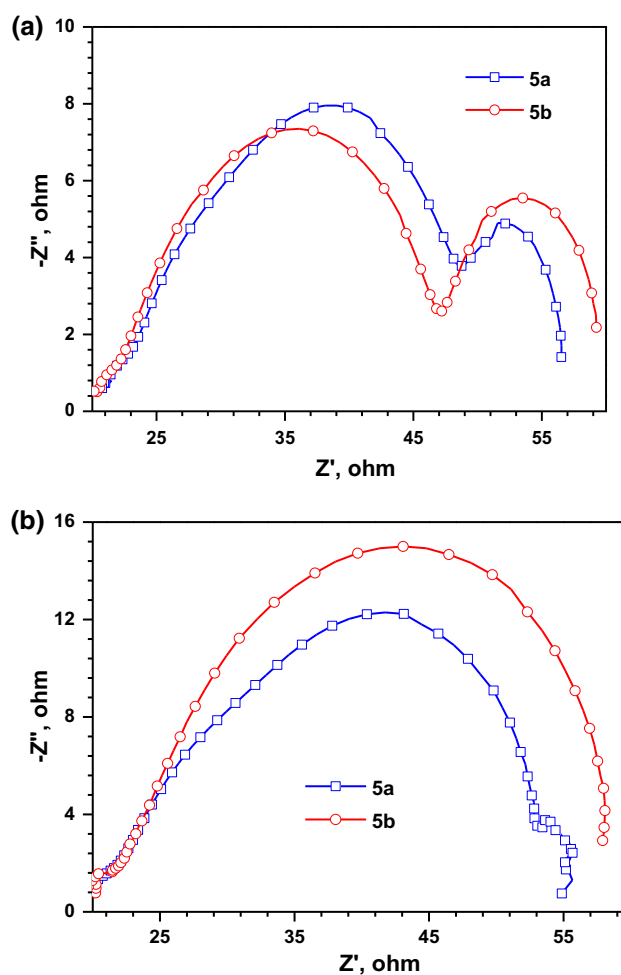
Fig. 10 Nyquist plots observed for the DSSCs fabricated using dyes under **a** dark and **b** illumination conditions

same as observed for V_{OC}. For the Nyquist plots under illumination, charge transfer resistance (R_{ct2}) shows the order **5a** > **5b** followed by the reference dyes **D1**–**D6**. This order is in agreement with the observed J_{SC} values for the set of present dyes and reference dyes.

The electron lifetime can be extracted from the angular frequency (ω_{min}) at the mid-frequency peak related to
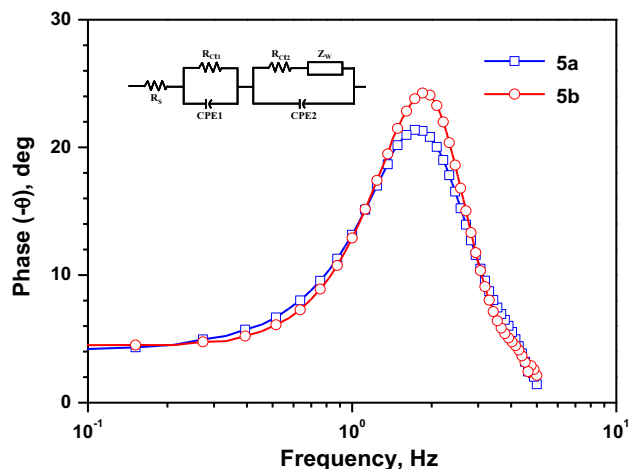
Fig. 11 Bode phase plots measured under illumination of the DSSCs fabricated using dyes

charge recombination in the Bode phase plot (Fig. 11) by using $\tau_e = 1/\omega_{min}$ [61]. The electron lifetime is a measure of suppression of back reaction of injected electrons with I_3^- in the electrolyte. The electron lifetime calculated from the plot follows a trend **5a > 5b**. This trend is similar to that shown by parent dyes **D1–D2** and reference dyes **D5–D6**. Also, the obtained τ_e values are consistent with the V_{OC} values for the dyes. It is believed that the large electron lifetime is essential to improve the J_{SC} and V_{OC} which subsequently enhances the power conversion efficiency of the DSSCs.

4 Conclusion

New D–π–A sensitizers containing fluorenylidene functionalized phenothiazine donor, cyanoacrylic acid as the acceptor/anchoring group, and fluorene and thiophene or bithiophene in the conjugation segment were synthesized and applied to DSSCs. Introduction of fluorenylidene chromophore as a peripheral antenna helps to enhance the light-harvesting capability of the sensitizers resulting in high molar extinction coefficients. Both the dyes presented in this work are found to be attractive for DSSCs since they possess high lying LUMO and low lying HOMO energies which enhances the electron injection into the conduction band and easy regeneration of the oxidized dye respectively. When employed to DSSCs they (**5a** and **5b**) led to a photocurrent density of 7.01 and 6.71 mA cm^{-2} and an open circuit voltage of 679 and 635 mV, respectively. The dye **5a** bearing fluorenylthiophene in the conjugation exhibited better efficiency (3.31 %) originating due to the relatively high V_{OC} which is attributed to enhanced resistance for recombination witnessed by elongated electron lifetime.

References

1. B. O'Regan, M. Grätzel, A low-cost, high-efficiency solar cell based on dye-sensitized colloidal TiO$_2$ films. Nature **353**, 737–740 (1991)
2. N.S. Lewis, Toward cost-effective solar energy use. Science **315**, 798–801 (2007)
3. A. Hagfeldt, G. Boschloo, L. Sun, L. Kloo, H. Pettersson, Dye-sensitized solar cells. Chem. Rev. **110**, 6595–6663 (2010)
4. T.W. Hamann, R.A. Jensen, A.B.F. Martinson, H. Van Ryswyk, J.T. Hupp, Advancing beyond current generation dye-sensitized solar cells. Energy Environ. Sci. **1**, 66–78 (2008)
5. M. Pagliaro, G. Palmisano, R. Ciriminna, V. Loddo, Nanochemistry aspects of titania in dye-sensitized solar cells. Energy Environ. Sci. **2**, 838–844 (2009)
6. J. Fang, H. Fan, H. Tian, G. Dong, Morphology control of ZnO nanostructures for high efficient dye-sensitized solar cells. Mater. Charact. **108**, 51–57 (2015)
7. A.B. Martinson, J.W. Elam, J.T. Hupp, M.J. Pellin, ZnO nanotube based dye-sensitized solar cells. Nano Lett. **7**, 2183–2187 (2007)
8. X. Zou, H. Fan, Y. Tian, M. Zhang, X. Yan, Chemical bath deposition of Cu$_2$O quantum dots onto ZnO nanorod arrays for application in photovoltaic devices. RSC Adv. **5**, 23401–23409 (2015)
9. M. Matsumura, Y. Nomura, H. Tsubomura, Dye-sensitization on the photocurrent at zinc oxide electrode in aqueous electrolyte solution. Bull. Chem. Soc. Jpn. **50**, 2533–2537 (1977)
10. N. Alonso, M. Beley, P. Chartier, V. Ern, Dye sensitization of ceramic semiconducting electrodes for photoelectrochemical conversion. Rev. Phys. Appl. **16**, 5–10 (1981)
11. J. Desilvestro, M. Grätzel, L. Kavan, J. Moser, Highly efficient sensitization of titanium dioxide. J. Am. Chem. Soc. **107**, 2988–2990 (1985)
12. A. Mishra, M.K.R. Fischer, P. Baüerle, Metal-free organic dyes for dye-sensitized solar cells: from structure: property relationships to design rules. Angew. Chem. Int. Ed. **48**, 2474–2499 (2009)
13. Y. Ooyama, Y. Harima, Photophysical and electrochemical properties, and molecular structures of organic dyes for dye-sensitized solar cells. ChemPhysChem **13**, 4032–4080 (2012)
14. Y. Ooyama, Y. Harima, Molecular designs and syntheses of organic dyes for dye-sensitized solar cells. Eur. J. Org. Chem. **18**, 2903–2934 (2009)
15. M.K. Nazeeruddin, P. Péchy, T. Renouard, S.M. Zakeeruddin, R. Humphry-Baker, P. Comte, P. Liska, L. Cevey, E. Costa, V. Shklover, L. Spiccia, G.B. Deacon, C.A. Bignozzi, M. Grätzel, Engineering of efficient panchromatic sensitizers for nanocrystalline TiO$_2$-based solar cells. J. Am. Chem. Soc. **123**, 1613–1624 (2001)
16. A. Yella, H.-W. Lee, H.N. Tsao, C. Yi, A.K. Chandiran, M.K. Nazeeruddin, E.W.-G. Diau, C.-Y. Yeh, S.M. Zakeeruddin, M. Grätzel, Porphyrin-sensitized solar cells with cobalt (II/III)—based redox electrolyte exceed 12% efficiency. Science **334**, 629–634 (2011)

17. M. Liang, J. Chen, Arylamine organic dyes for dye-sensitized solar cells. Chem. Soc. Rev. **42**, 3453–3488 (2013)

18. Z. Ning, H. Tian, Triarylamine: a promising core unit for efficient photovoltaic materials. Chem. Commun. **37**, 5483–5495 (2009)

19. C.-J. Yang, Y.J. Chang, M. Watanabe, Y.-S. Hon, T.J. Chow, Phenothiazine derivatives as organic sensitizers for highly efficient dye-sensitized solar cells. J. Mater. Chem. **22**, 4040–4049 (2012)

20. J. Tang, J. Hua, W. Wu, J. Li, Z. Jin, Y. Long, H. Tian, New starburst sensitizer with carbazole antennas for efficient and stable dye-sensitized solar cells. Energy Environ. Sci. **3**, 1736–1745 (2010)

21. Y. Wu, M. Marszalek, S.M. Zakeeruddin, Q. Zhang, H. Tian, M. Grätzel, W. Zhu, High-conversion-efficiency organic dye-sensitized solar cells: molecular engineering on D–A–π–A featured organic indoline dyes. Energy Environ. Sci. **5**, 8261–8272 (2012)

22. P. Yu, F. Zhang, M. Li, R. He, Influence of position of auxiliary acceptor in D-A–π–A photosensitizes on photovoltaic performances of dye-sensitized solar cells. J. Mater. Sci. **50**, 7333–7342 (2015)

23. H. Choi, C. Baik, S.O. Kang, J. Ko, M.S. Kang, M.K. Nazeeruddin, M. Grätzel, Highly efficient and thermally stable organic sensitizers for solvent-free dye-sensitized solar cells. Angew. Chem. **120**, 333–336 (2008)

24. Z. Wan, C. Jia, J. Zhang, Y. Duan, Y. Lin, Y. Shi, Triphenylamine-based starburst dyes with carbazole and phenothiazine antennas for dye-sensitized solar cells. J. Power Sources **199**, 426–431 (2012)

25. X. Jiang, K.M. Karlsson, E. Gabrielsson, E.M. Johansson, M. Quintana, M. Karlsson, L. Sun, G. Boschloo, A. Hagfeldt, Highly efficient solid-state dye-sensitized solar cells based on triphenylamine dyes. Adv. Funct. Mater. **21**, 2944–2952 (2011)

26. A. Baheti, K.R.J. Thomas, C.-T. Li, C.-P. Lee, K.-C. Ho, Organic dyes containing fluoren-9-ylidene chromophores for efficient dye-sensitized solar cells. J. Mater. Chem. A **2**, 5766–5779 (2014)

27. B. Liu, B. Wang, R. Wang, L. Gao, S. Huo, Q. Liu, X. Li, W. Zhu, Influence of conjugated π-linker in D–D–π–A indoline dyes: towards long-term stable and efficient dye-sensitized solar cells with high photovoltage. J. Mater. Chem. A **2**, 804–812 (2014)

28. D. Kuang, S. Uchida, R. Humphry-Baker, S.M. Zakeeruddin, M. Grätzel, Organic dye-sensitized ionic liquid based solar cells: remarkable enhancement in performance through molecular design of indoline sensitizers. Angew. Chem. Int. Ed. **47**, 1923–1927 (2008)

29. A. Venkateswararao, K.R.J. Thomas, C.-T. Li, K.C. Ho, Functional tuning of organic dyes containing 2,7-carbazole and other electron-rich segments in the conjugation pathway. RSC Adv. **5**, 17953–17966 (2015)

30. J.-F. Huang, J.-M. Liu, L.-L. Tan, Y.-F. Chen, Y. Shen, L.-M. Xiao, D.-B. Kuang, C.-Y. Su, Novel carbazole based sensitizers for efficient dye-sensitized solar cells: role of the hexyl chain. Dyes Pigments **114**, 18–23 (2015)

31. A. Venkateswararao, K.R.J. Thomas, C.-P. Lee, K.C. Ho, Synthesis and characterization of organic dyes containing 2,7-disubstituted carbazole π-linker. Tetrahedron Lett. **54**, 3985–3989 (2013)

32. A. Venkateswararao, K.R.J. Thomas, in *Solar Cell Nanotechnology*, vol. 2, ed. by A. Tiwari, R. Boukherroub, M. Sharon (Wiley-Scrivener, Beverly, 2014), pp. 41–96

33. A. Venkateswararao, K.R.J. Thomas, C.-P. Lee, C.-T. Li, K.C. Ho, Organic dyes containing carbazole as donor and π-linker: optical, electrochemical, and photovoltaic properties. ACS Appl. Mater. Interfaces **6**, 2528–2539 (2014)

34. G.B. Bodedla, K.R.J. Thomas, C.-T. Li, K.-C. Ho, Functional tuning of phenothiazine-based dyes by a benzimidazole auxiliary chromophore: an account of optical and photovoltaic studies. RSC Adv. **4**, 53588–53601 (2014)

35. A. Baheti, K.R.J. Thomas, C.-T. Li, C.-P. Lee, K.-C. Ho, Fluorene-based sensitizers with a phenothiazine donor: effect of mode of donor tethering on the performance of dye-sensitized solar cells. ACS Appl. Mater. Interfaces **7**, 2249–2262 (2015)

36. Y. Hua, S. Chang, H. Wang, D. Huang, J. Zhao, T. Chen, W.-Y. Wong, W.-K. Wong, X. Zhu, New phenothiazine-based dyes for efficient dye-sensitized solar cells: positioning effect of a donor group on the cell performance. J. Power Sources **243**, 253–259 (2013)

37. S. Wang, H. Wang, J. Guo, H. Tang, J. Zhao, Influence of the terminal electron donor in D–D–π–A phenothiazine dyes for dye-sensitized solar cells. Dyes Pigments **109**, 96–104 (2014)

38. B.N. Achar, M.A. Ashok, Electrical measurements and thermal kinetics study of phenothiazine and a few of its derivatives. Mater. Chem. Phys. **108**, 8–15 (2008)

39. S. Kumar, K.R.J. Thomas, C.-T. Li, K.-C. Ho, Synthesis and photovoltaic properties of organic dyes containing N-fluoren-2-yl dithieno[3,2-b:2′,3′-d]pyrrole and different donors. Org. Electron. **26**, 109–116 (2015)

40. L.E. Polander, A. Yella, J. Teuscher, R. Humphry-Baker, B.F.E. Curchod, N. Ashari, P. Peng Gao, J.-E. Moser, I. Tavernelli, U. Rothlisberger, M. Grätzel, M.K. Nazeeruddin, J. Julien Frey, Unravelling the potential for dithienopyrrole sensitizers in dye-sensitized solar cells. Chem. Mater. **25**, 2642–2648 (2013)

41. Z. Wang, M. Liang, Y. Tan, L. Ouyang, Z. Sun, S. Xue, Organic dyes containing dithieno[2,3-d:2′,3′-d']-thieno[3,2-b:3′,2′-b']dipyrrole core for efficient dye-sensitized solar cells. J. Mater. Chem. A **3**, 4865–4874 (2015)

42. K.R.J. Thomas, A. Baheti, Fluorene based organic dyes for dye sensitised solar cells: structure–property relationships. Mater. Technol. **28**, 71–87 (2013)

43. A. Baheti, S.R. Gajjela, P. Balaya, K.R.J. Thomas, Synthesis, optical, electrochemical and photovoltaic properties of organic dyes containing trifluorenylamine donors. Dyes Pigments **113**, 78–86 (2015)

44. A. Baheti, P. Singh, C.-P. Lee, K.R.J. Thomas, K.-C. Ho, 2,7-Diaminofluorene-based organic dyes for dye-sensitized solar cells: effect of auxiliary donor on optical and electrochemical properties. J. Org. Chem. **76**, 4910–4920 (2011)

45. M. Marszalek, S. Nagane, A. Ichake, R. Humphry-Baker, V. Paul, S.M. Zakeeruddin, M. Grätzel, Tuning spectral properties of phenothiazine based donor–p–acceptor dyes for efficient dye-sensitized solar cells. J. Mater. Chem. **22**, 889 (2012)

46. M.J. Frisch, G.W. Trucks, H.B. Schlegel, G.E. Scuseria, M.A. Robb, J.R. Cheeseman, G. Scalmani, V. Barone, B. Mennucci, G.A. Petersson, H. Nakatsuji, M. Caricato, X. Li, H.P. Hratchian, A.F. Izmaylov, J. Bloino, G. Zheng, J.L. Sonnenberg, M. Hada, M. Ehara, K. Toyota, R. Fukuda, J. Hasegawa, M. Ishida, T. Nakajima, Y. Honda, O. Kitao, H. Nakai, T. Vreven, J.A. Montgomery, J.E. Peralta, F. Ogliaro, M. Bearpark, J.J. Heyd, E. Brothers, K.N. Kudin, V.N. Staroverov, R. Kobayashi, J. Normand, K. Raghavachari, A. Rendell, J.C. Burant, S.S. Iyengar, J. Tomasi, M. Cossi, N. Rega, N.J. Millam, M. Klene, J.E. Knox, J.B. Cross, V. Bakken, C. Adamo, J. Jaramillo, R. Gomperts, R.E. Stratmann, O. Yazyev, A.J. Austin, R. Cammi, C. Pomelli, J.W. Ochterski, R.L. Martin, K. Morokuma, V.G. Zakrzewski, G.A. Voth, P. Salvador, J.J. Dannenberg, S. Dapprich, A.D. Daniels, O. Farkas, J.B. Foresman, J.V. Ortiz, J. Cioslowski, D.J. Fox, *Gaussian, Inc., Wallingford CT, Gaussian 09 (Revision-A. 02)* (Gaussian. Inc., Wallingford, 2009)

47. Y. Zhao, D.G. Truhlar, Density functionals with broad applicability in chemistry. Acc. Chem. Res. **41**, 157–167 (2008)

48. N. Godbout, D.R. Salahub, J. Andzelm, E. Wimmer, Optimization of gaussian-type basis-sets for local spin-density functional

calculations. Part I. Boron through neon, optimization technique and validation. Can. J. Chem. **70**, 560–571 (1992)

49. C. Sosa, J. Andzelm, B.C. Elkin, E. Wimmer, K.D. Dobbs, D.A. Dixon, A local density functional-study of the structure and vibrational frequencies of molecular transition-metal compounds. J. Phys. Chem. **96**, 6630–6636 (1992)

50. J.F. Hartwig, Transition metal catalyzed synthesis of arylamines and aryl ethers from aryl halides and triflates: scope and mechanism. Angew. Chem. Int. Ed. **37**, 2046–2067 (1998)

51. J.K. Stille, The palladium-catalyzed cross-coupling reactions of organotin reagents with organic electrophiles [new synthetic methods (58)]. Angew. Chem. Int. Ed. **25**, 508–523 (1986)

52. Y. Hua, S. Chang, D. Huang, X. Zhou, X. Zhu, J. Zhao, T. Chen, W.-Y. Wong, W.-K. Wong, Significant improvement of dye-sensitized solar cell performance using simple phenothiazine based dyes. Chem. Mater. **25**, 2146–2153 (2013)

53. K. Sayama, S. Tsukagoshi, K. Hara, Y. Ohga, A. Shinpou, Y. Abe, S. Suga, H. Arakawa, Photoelectrochemical properties of J aggregates of benzothiazole merocyanine dyes on a nanostructured TiO_2 film. J. Phys. Chem. B **106**, 1363–1371 (2002)

54. G. Li, K.-J. Jiang, Y.-F. Li, S.-L. Li, L.-M. Yang, Efficient structural modification of triphenylamine-based organic dyes for dye-sensitized solar cells. J. Phys. Chem. C **112**, 11591–11599 (2008)

55. M.K. Nazeeruddin, S.M. Zakeeruddin, R. Humphry-Baker, M. Jirousek, P. Liska, N. Vlachopoulos, V. Shklover, C.-H. Fischer, M. Grätzel, Acid-base equilibria of (2,2′-bipyridyl-4,4′-dicarboxylic acid)ruthenium(II) complexes and the effect of protonation on charge-transfer sensitization of nanocrystalline titania. Inorg. Chem. **38**, 6298–6305 (1999)

56. C. Reichardt, Solvatochromic dyes as solvent polarity indicators. Chem. Rev. **94**, 2319–2358 (1994)

57. A. Baheti, P. Tyagi, K.R.J. Thomas, Y.-C. Hsu, J.T. Lin, Simple triarylamine-based dyes containing fluorene and biphenyl linkers for efficient dye-sensitized solar cells. J. Phys. Chem. C **113**, 8541–8547 (2009)

58. A.N.M. Green, E. Palomares, S.A. Haque, J.M. Kroon, J.R. Durrant, Charge transport versus recombination in dye-sensitized solar cells employing nanocrystalline TiO_2 and SnO_2 films. J. Phys. Chem. B **109**, 12525–12533 (2005)

59. M. Grätzel, Photoelectrochemical cells. Nature **414**, 338–344 (2001)

60. X.-H. Zhang, Y. Cui, R. Katoh, N. Koumura, K. Hara, Organic dyes containing thieno[3,2-*b*]indole donor for efficient dye-sensitized solar cells. J. Phys. Chem. C **114**, 18283–18290 (2010)

61. J. van de Lagemaat, N.-G. Park, A.J. Frank, Influence of electrical potential distribution, charge transport, and recombination on the photopotential and photocurrent conversion efficiency of dye-sensitized nanocrystalline TiO_2 solar cells: a study by electrical impedance and optical modulation techniques. J. Phys. Chem. B **104**, 2044–2052 (2000)